Non-I) estructive Measurements for CMOS Devices

Using Charge Collection Techniques

Larry Edmonds, Gary Swift, and Allan Johnston
Jet l'repulsion Laboratory
California Institut e of Technology[1]
Mail Stop 303-220
4800 Oak Grow Drive
Pasadena, California 91109-8099

Abstract

Results of an experiment providing initial validation of the use of charge collection spectroscopy to measure the over-layer and epitaxial thickness and substrate diffusion length are given for several CMOS SRAM test devices.

1.1 NTRODUCTION

"1'here is increasing use of commercial parts in the Space radiation environment. Quite Cd-ten manufacturers are reluctant to disclose basic device information, such as whether a part is on bulk silicon or has an epitaxial layer, that would aid in identifying the devices most qualified for use in the space radiat ion environment. This paper will tend to validate a simple test method, based on charge collection techniques on the benchtop using naturally occurring radioactive alpha particle sources, that will measu re device over-kryer thickness, epi thickness, and substrate diffusion length.

Epi thickness is an important parameter influencing, for example, susceptibility to latchup. The over-]ayer thickness is less important, except for ions with rapidly changing LET. The substrate diffusion length is important because charge collected from an ion track can greatly exceed the charge liberated in the epi layer [1] by an amount dependent on this parameter [2]. This applies to all ions, heavy or light, so the diffusion length is important to charge collection in general. It will be shown that exposure to particle irradiation can reduce the diffusion length and greatly reduce collected charge.

II. THE MODEL

Dussault et al. [1] observed, from computer simulations and experimental data, that charge collected from ion tracks in reverse-biased epi diodes can greatly exceed the charge liberated in the epi layer. This observation inspired further investigations [2] which resulted in some conclusions and models for charge collection in general (funneling and diffusion). The model for the total (integrated in time from 0 to m) collected charge, which agrees very well with computer simulation results, is especially simple because it is not affected by funneling. Funneling may affect the time profile of charge collection but, for the simple epi diodes considered, it does not affect the total collected charge. The model states that collected charge consists of charge liberated in the epi layer plus an additional contribution that reaches the epi via cliff usion from the heavily doped substrate below. The collected charge from a given ion track depends on device over-layer thickness, epi thickness, and substrate diffusion length. C)ver-layer thickness is relevant to low energy ions because it slows them down before they reach the epi layer. The model predicts collected charge from a given track in terms of these three device parameters.

[1] The research described in this paper was carried out by the Jet Propulsion Laboratory, California institute of Technology, under a contract with the National Aeronautics and Space Administration, and supported by NASA Code-Q 1<1'01' funding.

Conversely, if collected charge is experimentally measured from alpha particles (which are convenient for this work) having a number of different energies, the device parameters can be estimated by fitting model predictions to data. This is the approach used for the present investigation.

Calculation of the charge liberated in the epi layer, Q_{epi}, is simple when using range-energy tables produced by the TRIM code [3]. The contribution, Q_{diff}, that diffuses from the substrate to the epi is calculated by dividing the track below the epi into many small sections. Let $\delta_i Q_{diff}$ be the amount of charge that diffuses to the epi when another amount $\delta_i Q$ is liberated a perpendicular distance y_i below the epi. The latter charge is calculated for each track section from the range-energy table provided by TRIM. When the substrate diffusion length, L_D, is small compared to substrate dimensions (almost always true for epi devices), simple diffusion theory produces the equation:

$$Q_{diff} = \sum \delta_i Q_{diff} = \sum \exp(-y_i/L_D)\, \delta_i Q$$

A simple computer code automates the calculations, and estimates the collected charge.

III. THE DEVICES

The devices tested are all versions of the Harris 11 S6516 CMOS (p-well) 16Kb SRAMs, which are denoted here as UNIRR9, IRRAD9, UNIRR12, IRRAD12, and MINIRR5. The numerical suffix in all cases refers to the initial grown epi thickness in pm. Processing should reduce each epi thickness by 3 to 5 pm [4]. A UNIRR and a IRRAD having the same suffix are identical except for different histories of particle exposure during earlier latchup investigations, Data presented later will show that these histories are relevant because they affect substrate diffusion length. The UNIRR (unirradiated) devices were not tested for latchup, while the IRRAD (irradiated) devices were extensively and repeatedly tested under various conditions (temperature, load resistance, etc.), resulting in a very large accumulated fluence from very heavy ions. Although accumulated total dose was considerable (about 36 Krads for the IRRAD9), the two IRRAD devices were still functional. The MINIRR (minimal irradiation) device was tested for latchup, but one test under the harshest latchup conditions determined that the device was immune, so no further tests were performed. Data presented later will indicate that the heavy-ion irradiation was not enough to significantly affect this device.

IV. Q VERSUS E CURVES

Charge collection measurements were performed using techniques pioneered by McNulty and his students [5,6]. A charge sensitive pre-amp is connected to the device and a histogram of the pulse distribution from ion hits is collected on a multi-channel analyzer (MCA). For the present cases, +5 volts was applied to the VCC pin with all other pins grounded. The pre-amp monitored current from the VCC pin. By measuring the sum of charges collected at all device nodes, the complexity associated with charge collected at one particular node is eliminated and the device simulates a large-arm diode in terms of charge collection characteristics.

Most data were obtained from a van de Graaff accelerator at the California Institute of I'ethnology (CIT). All tests used alpha particles because these particles are also available from a number of naturally occurring radioactive sources, making benchtop tests possible. For each device tested, collected charge Q was determined from MCA display peak centers and plotted against initial alpha particle energy E. Calibrations using a surface barrier detector were used to convert the M(.A peak center coordinate (channel number) into collected charge, At the lowest alpha particle energies (≈2 MeV), the peaks are fairly broad, as illustrated in Figure la for the UNIRR9. This is probably due to variations in over-layer thickness. The peaks are sharper at the higher energies, as illustrated in Figure 1b for the same device.

Measured Q versus E data for the UNIRR9 and IRRAD9 are shown as the circles in Figures 2 and 3. All of these data were obtained at (IT. It is immediately obvious from the measured data that the IRRAD9 collects much less charge from long-range tracks than the UNIRR9, indicating that particle irradiation from the latchup tests strongly affected the IRRAD9.

Some qualitative properties of Q versus E curves are easy to understand. At the lowest energies, the ion stops in or close to the epi layer, so collected charge is approximately proportional to the ion energy as it enters the epi. This explains the increase of Q with E at the

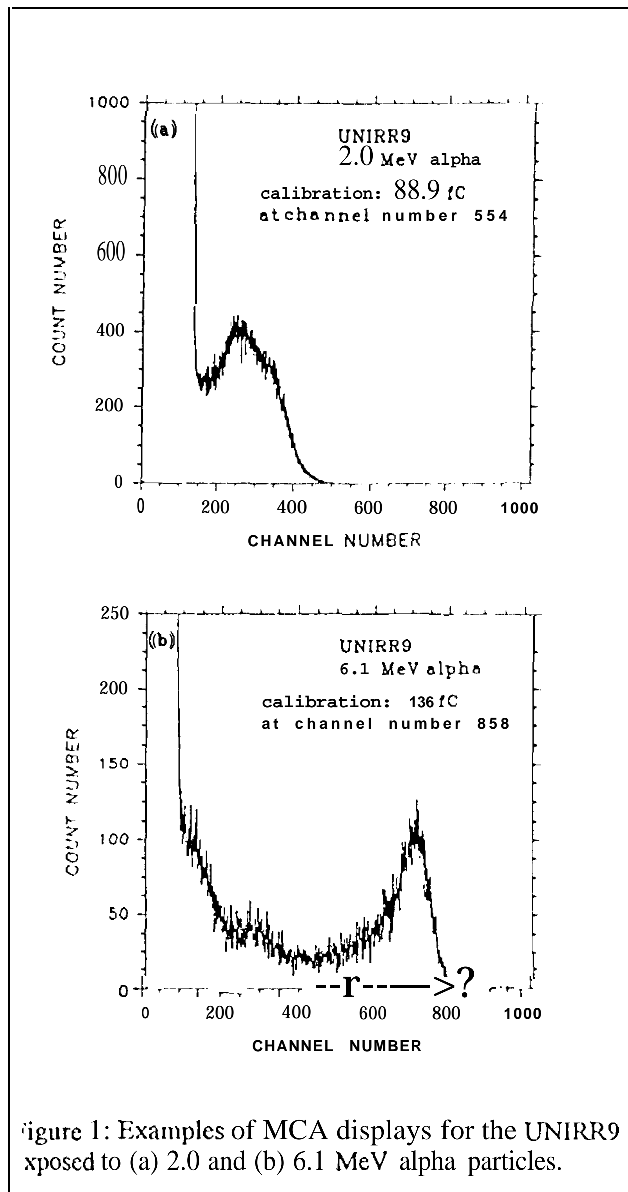

Figure 1: Examples of MCA displays for the UNIRR9 exposed to (a) 2.0 and (b) 6.1 MeV alpha particles.

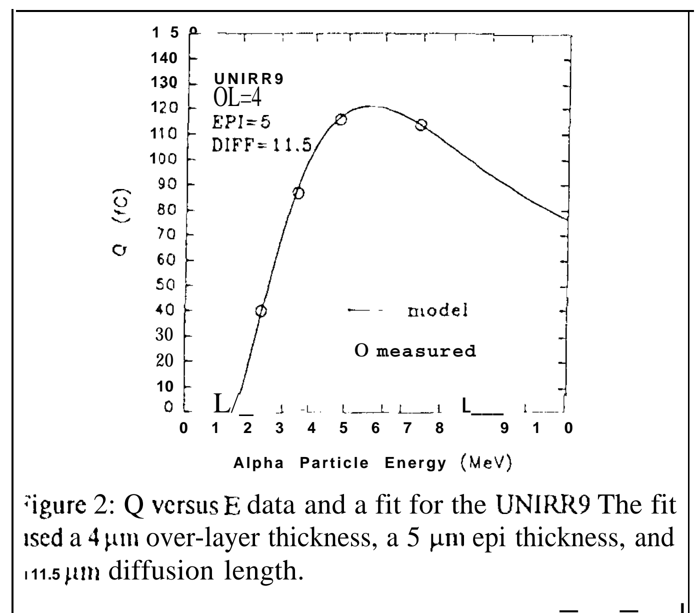

Figure 2: Q versus E data and a fit for the UNIRR9 The fit used a 4 µm over-layer thickness, a 5 µm epi thickness, and a 11.5 µm diffusion length.

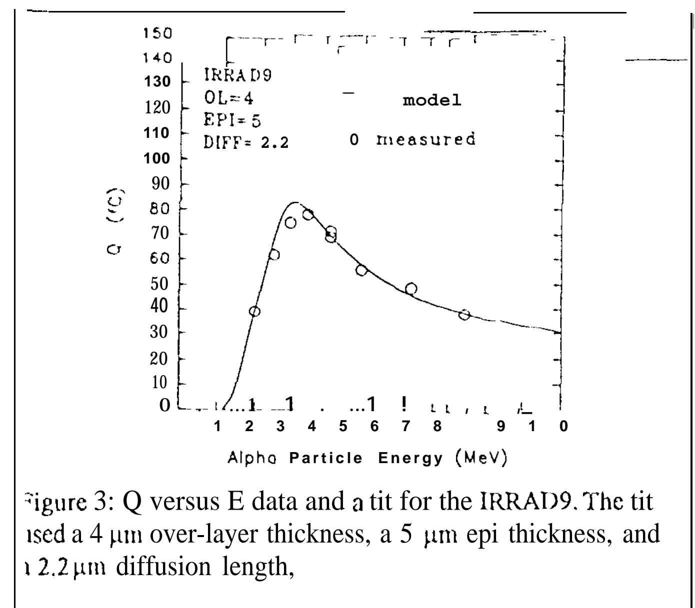

Figure 3: Q versus E data and a tit for the IRRAD9. The tit used a 4 µm over-layer thickness, a 5 µm epi thickness, and a 2.2 µm diffusion length,

lowest energies in Figures 2 and 3. At the highest energies, the track is long enough so that collected charge is primarily controlled by ion LET. The LET decreases with increasing E, and this explains the decreasing Q at the highest energies.

The solid curve in Figure 2 is the model prediction using over-layer thickness, epi thickness, and substrate diffusion length identified in the figures as OL, EPI, and DIFF, respectively (all in pm). All three parameters were adjusted to fit the data for the UNIRR9, and the result is OL=4, EPI=5, and DIFF=11.5 for this device. A post-processing epi thickness of about 5 µm was expected. Note that over-layer thickness includes all dead layers and is a Si equivalent, which will be larger than actual physical dimensions if there are any very dense structures. Furthermore, the devices were planerized, which also tends to increase over-layer thickness. Therefore the 4 µm estimate is reasonable.

The fit to the IRRAD9 shown in Figure 3 is a more severe test of the model. The postulate is that the IRRAD and UNIRR devices differ only because displacement damage from extensive latchup tests reduced the already small carrier lifetime in the IRRAD substrates. Therefore the IRRAD9 was assigned the same over-layer and epi thickness as the UNIRR9. Only one parameter (substrate diffusion length) was adjusted to fit all of the points in Figure 3. Note that the shape of the model predicted curve

is very different on opposite sides of the peak. It is encouraging that the data show the same behavior, and fit the curve very well in spite of only one adjustable parameter.

The relative importance of the two contributions to collected charge (Q_{epi} and Q_{diff}) can be seen by plotting the model predictions in different units. Instead of Q we use the ratio Q/Q_{epi}, and instead of E we use the depth of ion penetration below the over-layer. The results for the UNIRR9 and IRRAD9 are shown in Figures 4 and 5. Note that collected charge for the IRRAD9 from long-range tracks is mostly from the charge liberated in the epi, with a smaller contribution from the substrate. In contrast, the UNIRR9 collects a much greater amount of charge from long-range tracks, implying that much of this charge must be coming from the substrate.

Data and fits for the UNIRR12, IRRAD12, and MINIRR5 are shown in Figures 6, 7, and 8. The 6.1 MeV points for these devices were obtained from Cf252. All other points were obtained from the CIT accelerator. As before, the IRRAD is assigned the same OL and EPI as the UNIRR, so only one parameter was adjusted to fit the IRRAD 12 points. Note that model predictions fit data very well for each case. When combined with Figures 2 and 3, a consistent trend can be seen. Over-layer thickness is roughly the same for all devices. The post-processing epi thickness is 4 to 5 µm less than the pre-processing thickness for all devices. Both UNIRR devices have comparable substrate diffusion lengths, while the two IRRAD devices have much smaller diffusion lengths, The diffusion length for the MINIRR5 is almost the same as, but a little less than, those for the UNIRR devices, suggesting that the heavy-ion irradiation was not enough to significantly affect the MINIRR5.

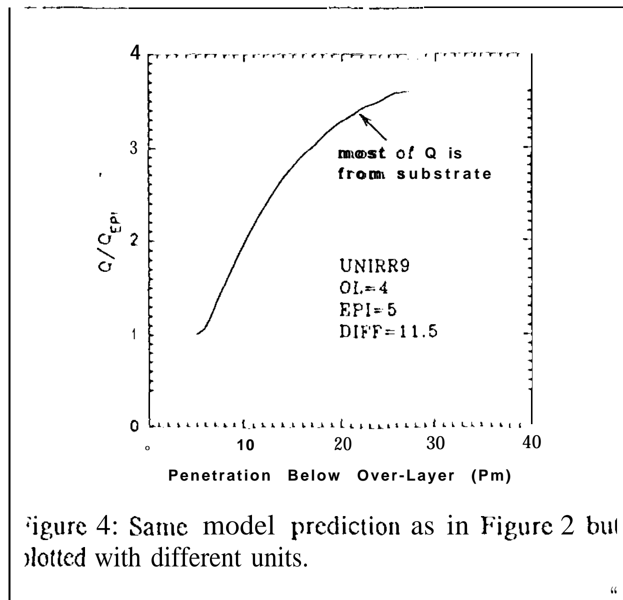

Figure 4: Same model prediction as in Figure 2 but plotted with different units.

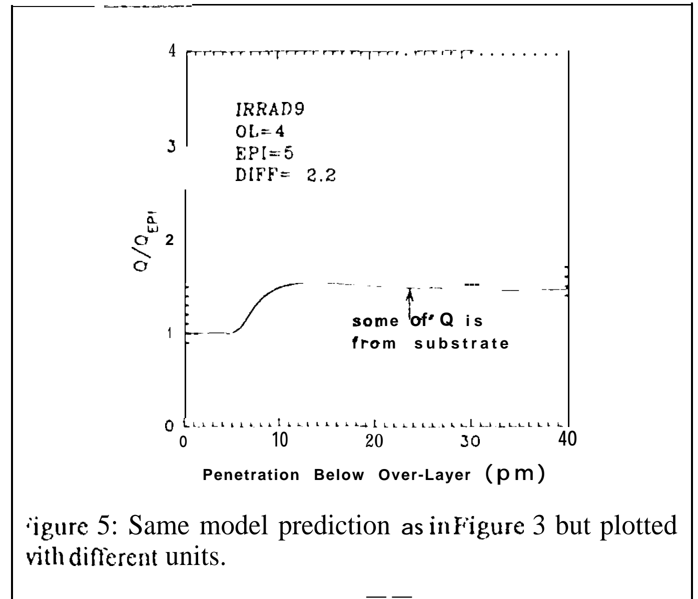

Figure 5: Same model prediction as in Figure 3 but plotted with different units.

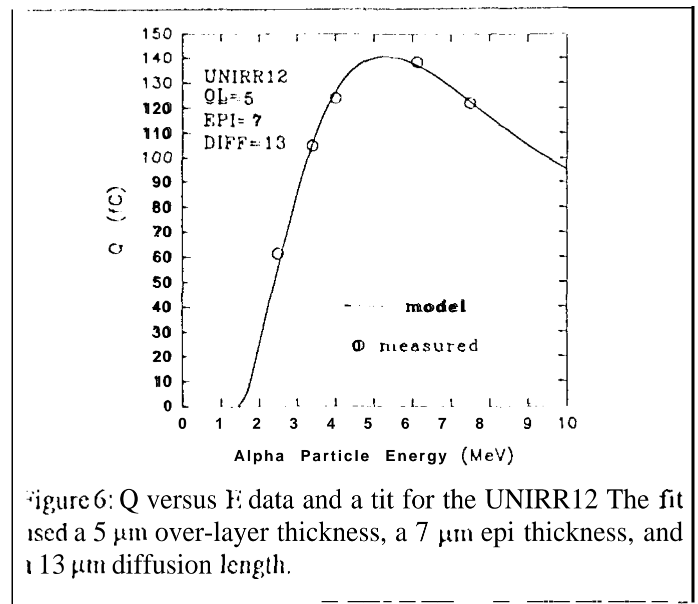

Figure 6: Q versus E data and a fit for the UNIRR12 The fit used a 5 µm over-layer thickness, a 7 µm epi thickness, and a 13 µm diffusion length.

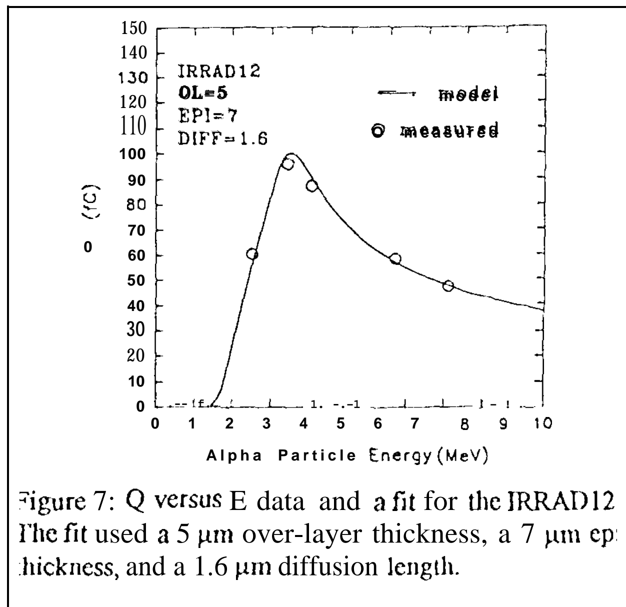

Figure 7: Q versus E data and a fit for the IRRAD12. The fit used a 5 μm over-layer thickness, a 7 μm epi thickness, and a 1.6 μm diffusion length.

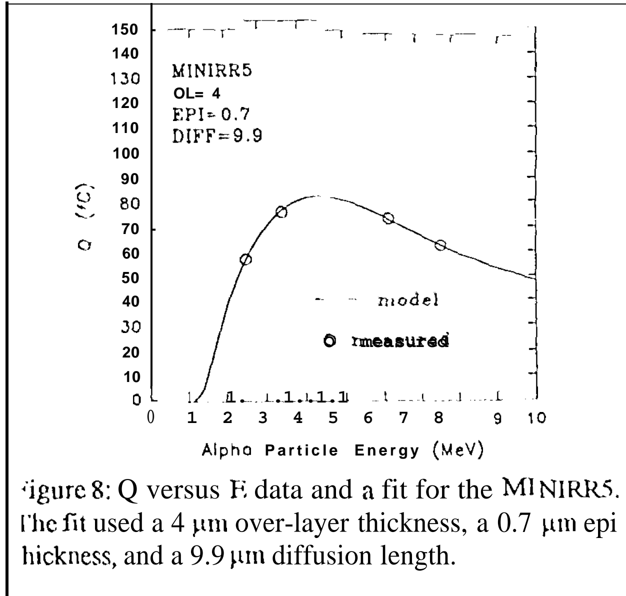

Figure 8: Q versus E data and a fit for the MINIRR5. The fit used a 4 μm over-layer thickness, a 0.7 μm epi thickness, and a 9.9 μm diffusion length.

V. SPECTRAL CURVES

Alpha particles from naturally occurring sources are obviously identical to those from an accelerator when both sources produce a narrow (in energy) spectrum centered at the same energy. The subject of naturally occurring sources becomes less trivial when the ion spectrum is distributed in energy. Such a distribution may occur from external mass shielding used to control ion energy, or from self-shielding in a source chosen to be thick enough to produce a given activity level. One monoenergic spectrum is needed to calibrate instrumentation but, having done that, it is possible to estimate device parameters using distributed sources. If the model can predict collected charge from each ion energy, than it can also predict a device response spectrum (a normalized count number versus Q, equivalent to an MCA display) from a known (measured) ion spectrum. The method of fitting predicted to measured device response spectrums (as opposed to Q versus E curves) will be called the spectral method.

A complication that the spectral method must address is that the device response has a distributed spectrum even when all alpha particles have exactly the same energy. This is, at least partly, because the device is not homogeneous and ion hits at different locations can produce different values of Q. When plotting Q versus E curves, the values of Q identified as measured are nominal values associated with peak centers. The spread in the device response was not an issue as long as peak centers are unambiguous. But this spread becomes an issue when using the spectral method because the spread from one ion energy can contaminate data produced by other energies. Examples of spread in the device response are shown in Figure 1. The figure shows two kinds of spread. One, which will be called the peak spread, is associated with the nonzero width of the peak. The other, which will be called the downward spread, is seen as counts at values of Q smaller than those contained in the peak. Downward spread contaminates data at values of Q smaller than the nominal value, but does not contaminate data at values of Q larger than the nominal value.

Peak spread can be included in the model predicted device response if it can be regarded as a known. It was empirically observed from the CIT data that this spread is roughly the same for different alpha particle energies until the energies are low enough (<3 MeV) so that variations in device over-layer thickness become an important contribution to the spread. To obtain a model predicted device response spectrum, it is necessary to estimate this spread using a >3 MeV monoenergic alpha particle source (e.g., the one used to calibrate instrumentation). The model prediction assumes that this same spread applies to all alpha particle energies. The model predicted device response spectrum can be expected to be narrower than the measured spectrum when the particle spectrum consists of low energy (<3 MeV) alpha particles.

The model prediction does not attempt to include downward spread. Because data from smaller values of Q are contaminated by downward spread from all larger

values of Q, agreement between model predicted and measured device response spectrums becomes progressively worse with decreasing Q. Therefore we should only look for agreement at the larger values of Q which are least affected by downward spread.

The alpha particle source used for the example to follow is Cf252. This sour-cc also produces heavy fission fragments, but these ions are clearly distinguishable from the alpha particles because the values of Q are greatly different. If amplifier gains are set for a convenient display of alpha particle hits on the MCA, hits from the fission fragments are off-scale and not even observable. Therefore the fission fragments are not a contamination problem, and Cf252 is a good alpha particle source for these measurements. Without shielding, the alpha particle spectrum is nearly monoenergic at about 6.12 MeV.

Although not normally recommended, shields made of paper (which are seen to be very inhomogeneous under magnification) are good for demonstrating that spread in the particle spectrum can be tolerated when the spectral method is used. Several measured particle spectrums are shown in Figure 9. The first (Figure 9a) is from the unshielded Cf. The second (Figure 9b) was obtained by shielding, the Cf with one ply separated from a paper towel. The third (Figure 9c) was produced by shielding the Cf with a two ply paper napkin, and the fourth (Figure 9d) used a thin piece of plastic wrapping material. The measured IRRAD 12 response spectrums are the dotted curves in Figure 10. These curves are the same as MCA displays (count number versus channel number) except that data were smoothed by averaging counts over bins containing eight channels, and unit conversions were used so that the result is a differential spectrum plotted against Q. The solid curves in Figure 10 are predictions obtained from the measured particle spectrums (but with instrumentation noise in channel numbers below 100 excluded, and with data smoothed by averaging over bins containing 8 channels), together with device parameters OL=4.4, EPI= 6.6, and DIFF= 2.0, selected to fit the measured data. These device parameter estimates are reasonably close to those obtained from the CIT data. As stated earlier, we only look for agreement between predicted and measured curves at the larger values of Q in Figure 10, because downward spread prohibits agreement at the smaller values. Furthermore, the predicted peak in Figure 10d is expected to be narrower than the measured peak, because the ion energies are low enough for variations in over-layer thickness to become observable.

Depending on the individual case, several ion spectrums may be nearly equivalent in terms of the information that they provide regarding the device. When this occurs, we may not be able to determine the three device parameters. For example, Figure 6 shows that all alpha particle energies between 5 and 6 MeV produce nearly the maximum Q for the UNIRR 12. The first three spectrums in Figure 9 all contain ions with these energies. For each of these ion spectrums, contributions to the device response spectrums at the largest values of Q come from the same ion energies. If we attempted to solve for the three UNIRR 12 parameters using the same steps just used for the IRRAD 12, we would find that we cannot, because many different pairs (EPI, DIFF) produce equally good fits. In order to avoid this problem, it is suggested that ion spectrum be fairly narrow and centered on each of several different energies. But the above example clearly shows that some spread in the ion spectrum can be tolerated if the spectral method is used. It should be adequate to use Cf252 shielded by each of several thicknesses of common materials, such as one or more layers of thin plastic wrapping materials.

VI. A POSSIBLE APPLICATION: DAMAGE ESTIMATES

A number of investigators do not (or did not) believe the postulate that heavy-ion irradiation from numerous latchup tests can produce enough displacement damage to change the substrate diffusion length. Note that the model predicted collected charge in Figure 3 for the IRRAD9 is mostly the charge liberated in a 5 μm thick region plus a smaller contribution that diffuses up to this region. It is difficult to imagine how the measured data can follow this rather erratic curve so well unless it really is true that collected charge is mostly the charge liberated in a 5 μm thick region. In contrast, Figure 2 shows that the UNIRR9 collects a much greater charge from long-range tracks, implying that much of it must come from far below this region. The data presented here may make the postulate easier to believe.

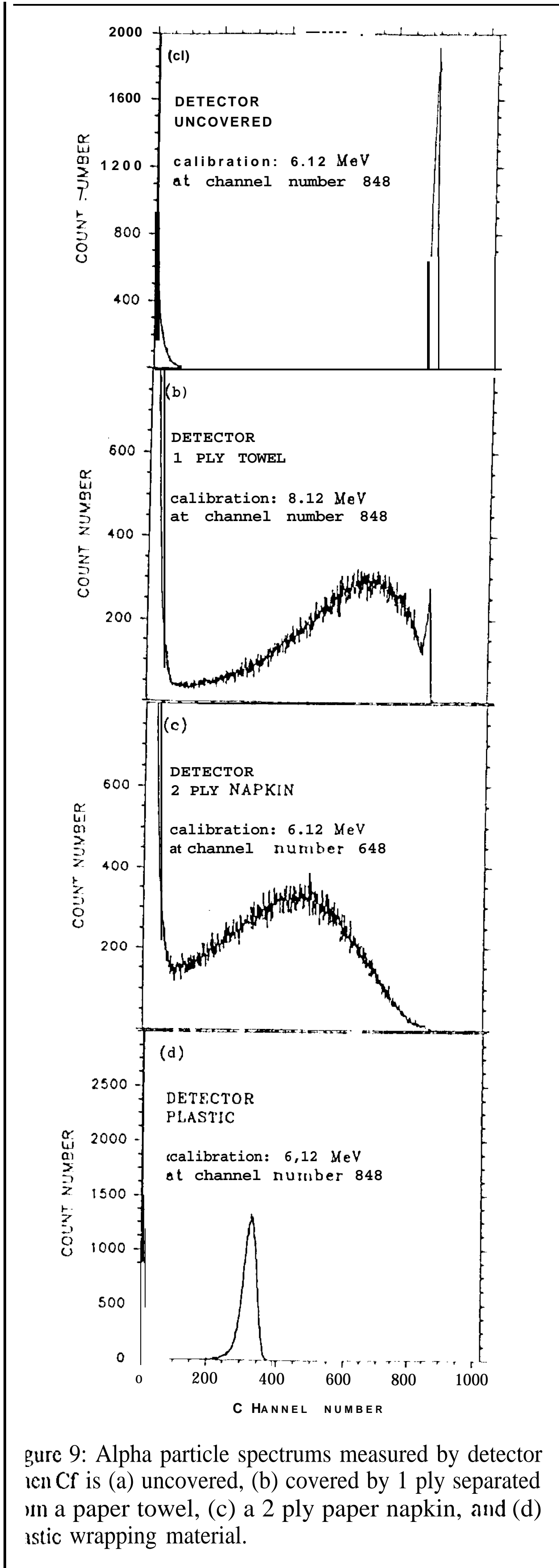

gure 9: Alpha particle spectrums measured by detector ıen Cf is (a) uncovered, (b) covered by 1 ply separated ım a paper towel, (c) a 2 ply paper napkin, and (d) ıstic wrapping material.

(a) IRRAD 12 UNCOVERED OL=4.4 EPI=6.6 DIFF=2.0 — model, measured

(b) IRRAD12 1 PLY TOWEL OL=4.4 EPI=6.6 DIFF=2.0 — model, measured

(c) IRRAD12 2 PLY NAPKIN OL=4.4 EPI=6.6 DIFF=2.0 — model, measured

(d) IRRAD12 PLASTIC OL=4.4 EPI=6.6 DIFF=2.0 — model, measured

DIFFERENTIAL SPECTRUM $(fC)^{-1}$

Q (fC)

gure 10: Measured IRRAD 12 response spectrum and a fit each ion spectrum shown in Figure 9. The fit used a 4.4 ı over-layer thickness, a 6.6 μm cpi thickness, and a 2.0 ı diffusion length.

Note that the density of defect centers should initially be greatest near the end of range of the ion. But these centers are mobile, until a reaction occurs which makes them stable [7], so diffusion will tend to make the density become more uniform. Furthermore, latchup tests were performed at a number of different incident angles, which also tends to make the density more uniform. It is not obvious just how uniform the density will become, and it is also not obvious how uniform the density needs to be in order to be approximated as uniform for the purpose of predicting device charge collection characteristics, But model predictions fit measured data extremely well, suggesting that the density is uniform enough for this purpose, at least for the two IRRAD devices considered here. This suggests that charge collection measurements, performed before and after irradiation (possibly at a number of different angles), might be used to determine an effective or average (defined in terms of charge collection) reduction in substrate diffusion length produced by a given amount and type of particle irradiation.

VII FUTURE WORK

We hope to include some other device types in the future. Of special interest are devices with p-type substrates, which may have longer substrate diffusion lengths. It will be interesting to determine how the two doping types compare with each other.

VIII CONCLUSIONS

The technique discussed in this paper provides a convenient and inexpensive approach to determine over-layer thickness, epi thickness, and substrate diffusion length. Epi thickness is an important parameter influencing, for example, susceptibility to latchup. Epi thickness and substrate diffusion length are both important to charge collection in general.

IX. REFERENCES

[1] H. Dussault, J.W. Howard Jr., R.C. Block, M.R. Pinto, W.J, Stapor, and A.R. Knudson, "High Energy Heavy-Ion-Induced Single Event Transients in Epitaxial Structures," *IEEE Trans. Nucl. Sci.*, *vol. 41*, no.6, pp.2018-2025, December 1994.

[2] L. Edmonds, "Charge Collection in Simple Epi Diodes," not yet published.

[3] J.F. Ziegler, *TRIM version* 95.4 *Instruction Manual,* IBM publication, March 1995.

[4] D. Takacs, J. Harter, E.P. Jacobs, C. Werner, U. Schwabe, J. Winnerl, and E. Lange, "Comparison of Latch-Up in P- and N-Well CMOS Circuits," *IEDM Technical Digest,* pp. 159-163, 1983.

[5] P.J. McNulty, D.R. Roth, W.J. Beauvais, W.G. Abdel-Kader, and D.C. Dinge, "Comparison of the Charge Collecting Properties of Junctions and the SEU Response of Microelectronic Circuits," *Nucl. Tracks and Radiat. Meas.*, vol. 19, nos. 1-4, pp.929-938, 1991.

[6] P.J. McNulty, W.J. Beavais, and D.R. Roth, "Determination of SEU Parameters of NMOS and CMOS SMMS," IEEE Trans. Nucl. Sci., vol.38, no.6, pp.1463-1470, December 1991.

[7] H.Y. Tada, J.R. Carter, Jr., B.E. Anspaugh, and R.G. Downing, *Solar Cell Radiation Handbook*, third edition, JPL Publication 82-69, p.3-9, November 1982.